International Journal of Pharmacology

Int. J. Pharmacol. **2026**; 22(5): 53974
https://doi.org/10.31083/IJP53974

Research Article

Integrative Analysis of Morphological, Phytochemical, and Genetic Variability in *Aloe* Species From the Taif Highlands of Saudi Arabia

Tarek M. Galal[1,*], Salma A. Aseeri[1], Eman Tawfik[2]

[1]Biology Department, College of Sciences, Taif University, 21944 Taif, Saudi Arabia
[2]Botany and Microbiology Department, Faculty of Science, Capital University, 11790 Cairo, Egypt
*Correspondence: t.aboseree@tu.edu.sa (Tarek M. Galal)
Academic Editor: Mehmet Ozaslan
Submitted: 5 March 2026 Revised: 27 June 2026 Accepted: 15 July 2026 Published: 20 September 2026

Abstract

Background: The genus *Aloe* comprises ecologically and pharmacologically important plants; however, the diversity of these taxa in the Arabian Peninsula remains incompletely characterized, particularly using integrative, multi-evidence frameworks. **Methods:** To our knowledge, this study provides, for the first time, a concurrent morphological, phytochemical, and molecular characterization of nine *Aloe* species collected from different locations in the Kingdom of Saudi Arabia (Taif, Al-Baha, Abha and Jazan), an ecologically significant yet under-researched region. Thus, this study aimed to elucidate interspecific diversity, establish chemotaxonomic relationships, and provide a robust foundation for conservation and pharmacological applications. **Results:** Comprehensive quantitative assessments of vegetative and reproductive morphological traits were recorded for all nine taxa. High-performance liquid chromatography (HPLC) was employed to detect and compare the accumulation profiles of seven major flavonoids, apigenin, luteolin, naringin, quercetin, rutin, kaempferol, and hesperetin, demonstrating species-specific phytochemical signatures with significant chemotaxonomic relevance. Molecular diversity was assessed using Random Amplified Polymorphic DNA (RAPD-PCR) with four decamer primers, which yielded 22 scorable bands and an overall polymorphism of 64.16%, indicating significant genetic differences among the species studied. Independent cluster and ordination analyses of morphological, phytochemical, and molecular datasets produced consistent species groupings, demonstrating that phenotypic, chemical, and genetic differentiation are mutually supportive and indicative of both evolutionary divergence and ecological adaptation to the environmental gradients of the Taif Highlands. **Conclusion:** The primary innovation of this study lies in the convergence of three distinct lines of evidence, creating a comprehensive reference framework for the taxonomy, conservation, and sustainable use of *Aloe* genetic and phytochemical resources in Saudi Arabia.

Keywords: *Aloe*; flavonoids; genetic variation; chemotaxonomy; high-performance liquid chromatography; phenylpropanoid biosynthesis

1. Introduction

Asphodelaceae is a natural (monophyletic) family; all its genera are considered to have evolved from a common ancestor [1]. The most obvious similarities among the genera are the succulent leaves, crescentiform or cymbiform leaf outlines, markedly bimodal karyotypes (2n = 14 chromosomes), the presence of 1-methyl-8-hydroxyanthraquinones in the roots and anthrone-C-glucosides in the leaves, and leaf vascular bundles containing a parenchymatous inner bundle sheath [2]. The genus *Aloe* occupies a central position in the taxonomy of Aloaceae because it is the first described genus and includes the largest number of species, and because it has been studied more extensively than other genera, both in taxonomy and systematics [3]. A reassessment of the classification of *Aloe* supports previous studies highlighting the need for taxonomic changes to reflect phylogenetic relationships between the core aloes and their sister groups [2,4].

The Kingdom of Saudi Arabia is the largest country in the Arabian Peninsula, located in western Asia. A major portion of Saudi Arabia is composed of sand desert, with the Rub' al-Khali being the largest sand desert in the world. However, in the southern and western parts of the country, there are several mountain ranges, some with peaks rising to almost 10,000 feet (3000 meters) above sea level. Owing to their higher rainfall and more favorable climates, these ranges support diverse ecosystems in which most of the *Aloe* species in Saudi Arabia occur [5]. Aloes are among the most familiar succulent plants globally, occupying a wide range of habitats and exhibiting various growth forms [6,7]. Aloes constitute an important component of the local flora of many countries from taxonomic, ethnomedicinal, chemical/chemotaxonomic, ecotouristic, and horticultural perspectives [8]. Consequently, this distinctive group of succulent plants generates wide-ranging interest among both scientists and plant collectors [8,9].

Flavonoids constitute a complex class of secondary metabolites widely distributed in plants, including the genus *Aloe*, where they play essential physiological and ecological roles. Flavonoids, such as apigenin, luteolin, kaempferol, rutin, naringin, and hesperetin, have been identified in *Aloe* species using high-performance liquid

chromatography (HPLC) and liquid chromatography–mass spectrometry (LC–MS) analyses [10,11]. These compounds function as powerful antioxidants, radical scavengers, and antibacterial agents, thereby enhancing the defenses of plants against oxidative stress, ultraviolet radiation, and infection [12,13]. Kaempferol is a prevalent flavonol found in approximately 80% of plant-based diets and plays a preventive role against lipid peroxidation and DNA damage [14]. In addition to their protective functions, flavonoids contribute to the chemotaxonomic differentiation of *Aloe* species, as quantitative and qualitative differences in flavonoid composition are often species-specific [15]. Variation in flavonoid profiles both supports the medicinal importance of *Aloe* and indicates adaptive biochemical responses to environmental stresses, rendering these metabolites essential for both ecological fitness and therapeutic potential [11].

Genetic variation among *Aloe* species is significant, reflecting evolutionary divergence and ecological adaptation. Molecular marker analyses, such as Random Amplified Polymorphic DNA (RAPD)-PCR, have been used effectively to assess genetic diversity among *Aloe* taxa, revealing polymorphism levels exceeding 65% in various studies [16,17]. The observed clustering patterns further illustrate the utility of RAPD markers in clarifying phylogenetic relationships and defining taxonomic boundaries within the genus *Aloe* [18]. Understanding this genetic diversity is essential for systematics, conservation, and the selection of elite genotypes for pharmaceutical and ecological applications.

Although the genus *Aloe* is known for its high medicinal and ecological importance, its diversity on the Saudi Arabian Peninsula remains poorly characterized. Previous research has typically relied on single lines of evidence, resulting in a limited understanding of how morphological differentiation, unique phytochemical markers, and genetic divergence converge. To address these gaps, the present study provides, to our knowledge, the first comprehensive simultaneous morphological, phytochemical, and molecular characterization of nine *Aloe* species collected from the neglected yet ecologically distinct Taif Highlands in southwestern Saudi Arabia. The aim was to integrate quantitative morphological assessments with HPLC profiles of seven major flavonoids to clarify interspecific diversity and chemotaxonomic relationships. Additionally, genetic divergence among the studied taxa was evaluated using RAPD-PCR markers. One of the primary innovations of this study is the use of pathway-anchored analysis to identify the enzymatic processes and environmental factors, such as ultraviolet (UV) radiation and aridity, that underlie species-specific metabolite profiles. Ultimately, the study aimed to establish a comprehensive reference framework for the taxonomy, conservation, and sustainable medicinal use of *Aloe* genetic and phytochemical resources in arid and semi-arid regions. More broadly, the study aimed to elucidate the evolutionary differentiation and ecological adaptability of *Aloe* species in dry and semi-arid environments to support their conservation, chemotaxonomic classification, and potential pharmaceutical applications.

2. Materials and Methods

Nine wild perennial *Aloe* species from different locations in the Kingdom of Saudi Arabia (Taif, Al-Baha, Abha, and Jazan) were collected for this study. These species were: *Aloe parvicoma* Lavranos & Collen., *Aloe* × *abhaica* Lavranos & Collen., *Aloe brunneodentata* Lavranos & Collen., *Aloe armatissima* Lavranos & Collen., *Aloe vera* var. *officinalis* (Forssk.) Baker, *Aloe sabaea* Schweinf., *Aloe castellorum* Wood, *Aloe fleurentiniorum* Lavranos & Newton, and *Aloe hijazensis* Lavranos & Collen. Identification and nomenclature were performed in accordance with Chaudhary [19] and as mentioned in Galal et al. [10]. Voucher specimens were deposited in the Taif University Herbarium.

2.1 Morphological Measurements

Morphological measurements were recorded for three individuals from each of the nine species to assess the main differences among them. Quantitative morphological traits were recorded from three mature, field-accessible individuals per species. Measurements were taken independently for each individual and are reported as mean ± standard deviation. These measurements included plant height, leaf length, leaf width at the widest point, tooth color and length, distance between teeth, rachis length, and flower length.

2.2 Estimation of Selected Phytochemical Compounds

HPLC combined with mass spectrometry (HPLC–MS) was utilized for the separation and quantification of flavonoids in the examined *Aloe* species. Three replicates were used for this assay, and samples were selected at random. All samples were of nearly the same age at the time of collection; they were wild plants collected at the flowering stage. Fresh leaf material from each species was collected, immediately frozen at −20 °C, and lyophilized before extraction. For each species, a representative pooled sample was prepared by combining equal dry-weight contributions from the three collected individuals to produce a single composite extract, thereby minimizing within-species variation and maximizing representativeness. This approach is consistent with standard practice for comparative phytochemical profiling of wild-collected plant material [15]. Each composite extract was then analyzed in triplicate technical replicates (n = 3 injections per species extract), and results are reported as means with a coefficient of variation (CV%) to indicate analytical reproducibility.

Flavonoid profiles (apigenin, luteolin, kaempferol, rutin, quercetin, naringin, hesperetin) were analyzed across nine *Aloe* taxa and collection localities. To contextualize potential chemotypes, site-level climate for the collec-

tion season was compiled from climatic data for matched weeks (±3–5 days) of UV index, air temperature, and daily precipitation. The coordinates for each locality were confirmed and mapped in Python (3.11.9, Python Software Foundation, Wilmington, DE, USA), providing a reproducible workflow for filtering unnecessary data, handling geographic coordinates, and plotting.

Pathway assignments followed Kyoto Encyclopedia of Genes and Genomes (KEGG) reference maps: phenylpropanoid (map00940; https://www.kegg.jp/pathway/map00940) and Flavone and flavonol (map00944; https://www.kegg.jp/pathway/map00944). Enzyme evidence used Enzyme Commission (EC) definitions with links:

phenylalanine ammonia-lyase (PAL) (EC 4.3.1.24; https://iubmb.qmul.ac.uk/enzyme/EC4/3/1/24.html),

C4H (EC 1.14.14.91; https://iubmb.qmul.ac.uk/enzyme/EC1/14/14/91.html),

4CL (EC 6.2.1.12; https://iubmb.qmul.ac.uk/enzyme/EC6/2/1/12.html),

chalcone synthase (CHS) (EC 2.3.1.74; https://iubmb.qmul.ac.uk/enzyme/EC2/3/1/74.html),

chalcone isomerase (CHI) (EC 5.5.1.6; https://enzyme.expasy.org/EC/5.5.1.6),

flavanone 3-hydroxylase (F3H) (EC 1.14.11.9; https://enzyme.expasy.org/EC/1.14.11.9),

FNS I (EC 1.14.20.5; https://iubmb.qmul.ac.uk/enzyme/EC1/14/20/5.html),

FNS II (EC 1.14.19.76; https://enzyme.expasy.org/EC/1.14.19.76),

flavonol synthase (FLS) (EC 1.14.20.6; https://iubmb.qmul.ac.uk/enzyme/EC1/14/20/6.html),

flavonoid 3′-hydroxylase (F3′H) (EC 1.14.14.82; https://iubmb.qmul.ac.uk/enzyme/EC1/14/14/82.html),

7-O-UGT (EC 2.4.1.185; https://iubmb.qmul.ac.uk/enzyme/EC2/4/1/185.html),

3-O-UGT (EC 2.4.1.91; https://iubmb.qmul.ac.uk/enzyme/EC2/4/1/91.html),

flavonol 3-O-glucoside 6″-O-rhamnosyltransferase (1,6-RhaT; EC 2.4.1.159, https://iubmb.qmul.ac.uk/enzyme/EC2/4/1/159.html),

flavanone 7-O-glucoside 2″-O-rhamnosyltransferase (1,2-RhaT; EC 2.4.1.236, https://iubmb.qmul.ac.uk/enzyme/EC2/4/1/236.html), and

flavonoid 4′-O-methyltransferase (F4′-OMT; EC 2.1.1.231, https://iubmb.qmul.ac.uk/enzyme/EC2/1/1/231.html).

Protein-domain context used InterPro entries:

2-oxoglutarate/Fe(II) oxygenases (IPR005123; https://www.ebi.ac.uk/interpro/entry/interpro/IPR005123),

cytochrome P450 (IPR001128; https://www.ebi.ac.uk/interpro/entry/interpro/IPR001128),

UDP-glucuronosyl/UDP-glucosyltransferases (IPR002213; https://www.ebi.ac.uk/interpro/entry/interpro/IPR002213), and

O-methyltransferase-like (IPR016461; https://www.ebi.ac.uk/interpro/entry/interpro/IPR016461).

Using these references, a rule-based mapping was implemented to convert the observed metabolite set for each species into the minimal viable enzyme complement consistent with the observed profile. This procedure yielded species-level network phenotypes.

2.3 Molecular Genetic Study (RAPD-PCR)

Genomic DNA was extracted from young *Aloe* leaves utilizing a modified Cetyle trimethylammonium bromide (CTAB) method to eliminate excess polysaccharides and polyphenols. Leaves were cryogenically frozen in liquid nitrogen, pulverized into a fine powder, and incubated in a CTAB extraction buffer enriched with high salt and polyvinylpyrrolidone (PVP) to sequester phenolics. Following chloroform: isoamyl alcohol extraction, DNA was precipitated with ice-cold absolute ethanol, washed, and resuspended in Tris Ethylenediaminetetraacetic acid (Tris-EDTA) (TE) buffer. DNA quality and yield were evaluated using A260/280 ratios and agarose gel electrophoresis to confirm the presence of high-molecular-weight DNA suitable for PCR applications [16].

For RAPD analysis, individual 10-mer primers (OPA-01, OPA-13, OPB-17, OPD-15) were used in 25 µL reactions containing approximately 25–50 ng of template DNA, 12.5 µL PCR master mix, 0.5 µM primer, and sterile ddH_2O, for a final volume of 25 µL. PCR conditions consisted of an initial denaturation at 95 °C for 5 minutes, followed by 35 cycles of 94 °C for 30 seconds, annealing at approximately 32–34 °C for 30 seconds, and extension at 72 °C for 1 minute, followed by a final extension at 72 °C for 10 minutes. RAPD profiles were resolved on 1.6% agarose gels, stained with ethidium bromide, and scored as presence/absence bands for genetic analysis [17].

The polymorphic information content (PIC) is a standard metric for evaluating the discriminatory power of molecular markers, and its inclusion strengthens the genetic analysis. For dominant binary markers, the PIC is calculated using the formula:

$$PIC = 1 - [f^2 + (1 - f)^2]$$

where f is the frequency of the presence allele across the taxa surveyed.

2.4 Data Analysis

The matrix of morphological, chemical, and molecular characteristics of the study species was analyzed using PAST (free software available online) [20]. Similarity of quantitative data was calculated using the Nei and Li/Dice similarity index, and similarity estimates were analyzed using unweighted pair group method using arithmetic averages (UPGMA). Agglomerative hierarchical clustering (UPGMA) and Wisconsin polar ordination were performed using PAST (Paleontological Statistics) software, version 4.03, according to Hammer et al. [21], freely available at https://www.nhm.uio.no/english/research/resources/past/.

3. Results

3.1 Morphological Charactristics

The morphological measurements of the nine *Aloe* species examined in the present study are presented in Table 1. The results showed clear variation in tooth color along the leaf margin, with all species bearing marginal teeth of different colors except *A. fleurentiniorum*, which is toothless and has an entire margin. In addition, three species (*A. parvicoma*, *A. brunneodentata*, and *A. castellorum*) had brown teeth, four species (*A. armatissima*, *A. vera* var. *officinalis*, *A. hijazensis*, and *A. sabaea*) had white teeth with a brown tip, and one species (*A. abhaica*) had green teeth with a brown tip. These observations are consistent with the description of the Flora of Saudi Arabia [19]. Plant height varied markedly from 15 cm in *A. brunneodentata* to 147 cm in *A. sabaea*. Regarding leaf morphology, *A. abhaica* had the longest leaves (66.0 cm), whereas *A. armatissima* had the widest (9.3 cm). In contrast, *A. brunneodentata* had the shortest leaves (11.3 cm), and *A. fleurentiniorum* had the narrowest (2.3 cm). The present study also revealed pronounced variation in leaf margin morphology among the *Aloe* species studied. Meanwhile, the longest marginal teeth (0.4 cm) were recorded in *A. parvicoma*, *A. brunneodentata*, and *A. vera* var. *officinalis*, whereas the shortest teeth (0.1 cm) were recorded in *A. castellorum*. As noted, *A. fleurentiniorum* was the only toothless species. Based on reproductive characters, *A. hijazensis* had the longest rachis (144 cm), while *A. fleurentiniorum* had the shortest (38 cm). The rachis of *A. abhaica* was the most branched, with nine branches, whereas those of *A. hijazensis*, *A. vera* var. *officinalis*, and *A. parvicoma* were the least branched, with two branches. Moreover, flower length varied considerably among the species: *A. armatissima* had the longest flowers (3.5 cm), whereas *A. parvicoma* had the shortest (2.6 cm).

3.2 Clustering Analysis of Morphological Data

The dendrogram derived from agglomerative clustering of the morphological characteristics of the nine *Aloe* species indicated that *A. castellorum* and *A. hijazensis* were the most similar taxa (Fig. 1). Five main groups were distinguished: (A) included *A. brunneodentata*, *A. parvicoma*, and *A. fleurentiniorum*; (B) comprised *A. abhaica* and *A. vera* var. *officinalis*; (C) included *A. hijazensis* and *A. castellorum*; (D) included *A. armatissima*; and (E) included *A. sabaea.* Furthermore, the Wisconsin polar ordination corroborated this grouping pattern, confirming the segregation of the study species into the same five clusters (Fig. 2). The heat map showed high morphological variation across all examined *Aloe* species for all evaluated variables (Fig. 3). The greatest plant heights were recorded for *A. sabaea* and *A. armatissima*, whereas the longest rachis length was recorded for *A. hijazensis* and *A. castellorum*. Conversely, *A. fleurentiniorum* exhibited the lowest values for several traits, especially leaf width, tooth length, and distance between teeth, indicating strong morphological divergence among the species.

3.3 High-Performance Liquid Chromatography (HPLC)

The production and variation of secondary metabolites, such as flavonoids, play a significant role in enabling plants to adapt to and thrive under diverse environmental conditions [22]. Generally, to determine the amount of an active component or marker compound present in a crude extract or derived preparation, a chromatographic technique such as HPLC requires a reference material as an external standard [23]. Thus, this study used quercetin to determine flavonoids. The total flavonoid content was previously estimated by Galal et al. [11]. HPLC data for the nine *Aloe* species examined identified seven flavonoid compounds with distinct retention times (RTs) (Table 2). These compounds were apigenin (RT = 18 min), luteolin (RT = 26 min), naringin (RT = 33 min), quercetin (RT = 40 min), rutin (RT = 43 min), kaempferol (RT = 51 min), and hesperetin (RT = 59 min).

Limit of detection (LOD) and limit of quantification (LOQ): LOD and LOQ were determined using the signal-to-noise ratio approach, with S/N = 3 for LOD and S/N = 10 for LOQ, in accordance with ICH Q2(R1) analytical validation guidelines. LOD values ranged from 0.05 to 0.12 µg/mL and LOQ values from 0.15 to 0.38 µg/mL, demonstrating sufficient sensitivity to detect and quantify all flavonoids at the concentrations present in the study extracts.

3.4 Mechanistic Contextualization of Flavonoid Profiles

Across nine taxa, metabolite profiles mapped onto a unified phenylpropanoid–flavonoid pathway resolve primarily into differences in branch choice and conjugation capacity (Fig. 4). The relatively high accumulation of apigenin in *A. parvicoma* is consistent with a metabolic flux favoring the flavone branch of the pathway, which in the phenylpropanoid–flavonoid network is associated with flavone synthase (FNS I/II) activity, whereas widespread luteolin indicates substantial F3′H activity acting on either apigenin or along the naringenin–eriodictyol route. Kaempferol accumulation, prominent in *A. sabaea* and *A. armatissima*, is consistent with robust F3H and FLS activities and limited diversion toward 3′-hydroxylated flavonols. The quercetin glycosylation ladder is species-specific: high rutin in *A. hijazensis* and *A. parvicoma* implies effective 3-O-UGT followed by 1,6-rutinosyltransferase, whereas its absence in *A. castellorum* and *A. vera* var. *officinalis* indicates a rutinosyltransferase bottleneck. Elevated naringin in *A. armatissima*, *A. castellorum*, and *A. sabaea* reflects strong 7-O-glucosyltransferase and 1,2-rhamnosyltransferase activities. Hesperetin was detected only in *A. parvicoma*, indicating an active F4′-O-methyltransferase acting on an F3′H-derived eriodictyol pool. Network constraints appear

Table 1. Morphological measurements of the nine studied *Aloe* species.

Species	Morphological variable								
	Plant height (cm)	Leaf length (cm)	Leaf width (cm)	Teeth length (cm)	Teeth distance (cm)	Rachis length (cm)	No. of rachis branches	Flower length (cm)	Teeth color
Aloe parvicoma	36	37.0	7.2	0.4	1.5	52	2	2.6	Brown
Aloe abhaica	63	66.0	8.3	0.3	1.6	94	9	3.4	Green with brown tip
Aloe brunneodentata	15	11.3	5.4	0.4	0.5	55	6	3.4	Brown
Aloe armatissima	122	37.3	9.3	0.2	1.4	121	5	3.5	White with brown tip
Aloe vera var. *officinalis*	57	39.0	4.9	0.4	1.0	77	2	2.7	White with brown tip
Aloe sabaea	147	56.7	6.9	0.2	0.8	49	3	3.4	White with brown tip
Aloe castellorum	49	35.3	6.6	0.1	1.3	140	4	3.2	Brown
Aloe fleurentiniorum	25	17.7	2.3	0	0.0	38	6	2.9	Entire margin
Aloe hijazensis	37	29.7	5.7	0.3	0.5	144	2	3.1	White with brown tip

Maximum and minimum values are underlined.

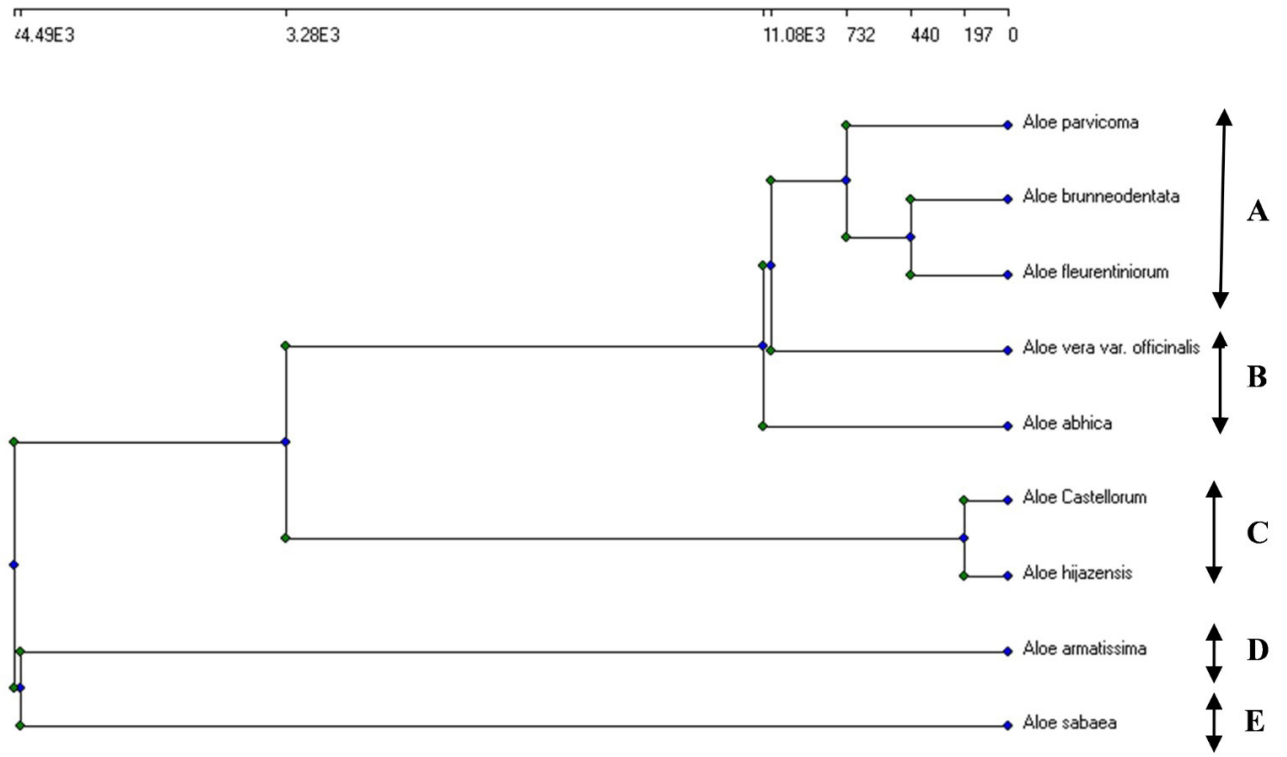

Fig. 1. Dendrogram obtained from agglomerative clustering of the morphological characteristics of the nine *Aloe* species examined in this study. In Fig. 1, Group A includes *Aloe brunneodentata*, *A. parvicoma*, and *A. fleurentiniorum*, indicating relatively similar overall morphological characteristics. Group B comprises *A. abhaica* and *A. vera* var. *officinalis*, reflecting similarities in their vegetative and reproductive traits. Group C includes *A. hijazensis* and *A. castellorum*, which represent the most morphologically similar species among the nine studied taxa. In contrast, Groups D and E consist individually of *A. armatissima* and *A. sabaea*, respectively, indicating its distinctive morphological characteristics and greater separation from the other species.

Table 2. Identified flavonoid compounds detected by high-performance liquid chromatography (HPLC) from the study of *Aloe* species.

Peak	Compound	RT (min)
1	Apigenin	18
2	Luteolin	26
3	Naringin	33
4	Quercetin	40
5	Rutin	43
6	Kaempferol	51
7	Hesperetin	59

RT, retention time.

broadly consistent across species. The lack of flavones in *A. abhaica* is explained by limited or absent FNS activity, whereas high rutin with minimal flavones in *A. hijazensis* reflects efficient quercetin conjugation. Competition between F3′H and FLS manifests as reciprocal trends in rutin (quercetin-derived) versus kaempferol: species favoring F3′H and downstream glycosylation accumulate rutin, whereas those favoring F3H/FLS accumulate kaempferol. Endpoint visibility is set by conjugation strength: when 3-O-UGT and 1,6-rutinosyltransferase are highly active, quercetin is chiefly observed as rutin; when rutinosylation is weak, quercetin pools persist as non-rutinosylated glucosides or other conjugates. Overall, branch-defining enzymes (FNS, F3H, FLS, F3′H) determine the aglycone spectrum, whereas tailoring modules (UGTs, rhamnosyltransferases, O-methyltransferases) determine the observed glycoside and methylated endpoints.

Notably, the flavonoid profiles reported here represent net accumulation levels detected by HPLC, which reflect the integrated effects of biosynthesis, modification, transport, and degradation. Inferences regarding enzymatic flux are therefore necessarily indirect and should be understood as hypotheses consistent with established pathway architecture according to Mao et al. [24] rather than as demonstrated biochemical conclusions. Environmental variables, including the UV index and precipitation gradients documented across collection sites, are acknowledged as co-determinants of metabolite accumulation alongside enzymatic capacity [22].

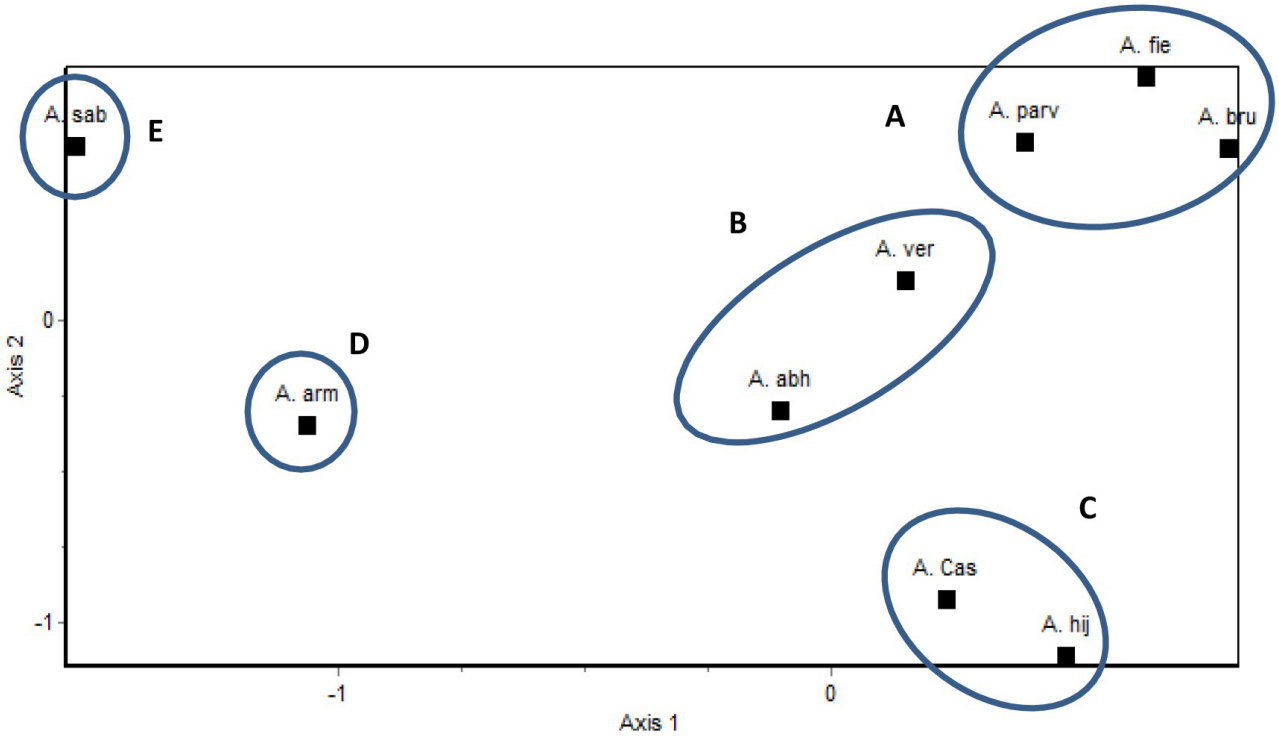

Fig. 2. Ordination plot based on non-metric similarity analysis of the morphological characteristics of the nine study *Aloe* species examined in this study. Fig. 2 shows the separation of the nine *Aloe* species into five distinct morphological groups. Group A includes *A. brunneodentata*, *A. parvicoma*, and *A. fleurentiniorum*, which share relatively similar overall morphological characteristics despite differences such as the toothless leaf margin of *A. fleurentiniorum*. Group B comprises *A. abhaica* and *A. vera* var. *officinalis*, indicating similarities in their vegetative and reproductive traits. Group C contains *A. hijazensis* and *A. castellorum*, representing the closest morphological relationship among the studied species. In contrast, Groups D and E consist individually of *A. armatissima* and *A. sabaea*, respectively, reflecting their distinct morphological characteristics. Overall, the ordination analysis confirms the clustering pattern and demonstrates considerable morphological diversity among the nine studied *Aloe* species.

Phenylpropanoid–Flavonoid Network Phenotypes in Aloe Across Contrasting Environments

A compound–enzyme–domain network integrated the *Aloe* dataset into a mechanistic framework with a shared upstream core (PAL–C4H–4CL–CHS–CHI) that feeds three branch modules (Fig. 5). Flavone outputs (apigenin, luteolin) map to flavone synthase (FNS I/II), with optional 3′-hydroxylation by F3′H; flavonol outputs (kaempferol, quercetin→rutin) require F3H and FLS followed by 3-O-UGT and 1,6-rhamnosyltransferase; flavanone glycosides (prunin→naringin) depend on 7-O-UGT and 1,2-rhamnosyltransferase. Domain clustering explains family-level constraints and multifunctionality: FNS I, F3H, and FLS coalesce within the 2-oxoglutarate/Fe(II) oxygenase family (IPR005123); FNS II, F3′H, and C4H cluster as cytochrome P450s (IPR001128); glycosyltransferases fall under IPR002213; O-methyltransferase activity maps to IPR016461. Competition for the naringenin node distinguishes flavone from flavonol routing, matching inverse trends between luteolin and rutin.

Projecting species profiles onto this network yielded distinct phenotypes. *A. parvicoma* shows a dominant FNS, moderate F3′H, and an active O-methyltransferase (hesperetin) capacity, but a weak flavanone-glycosylation arm. *A. armatissima* exhibits broad activation: high FNS and FLS, coupled with very strong 7-O-UGT/1,2-RhaT activities (largest naringin pool), while rutinosylation is present but not maximal. *A. castellorum* favors luteolin and naringin yet lacks rutin, diagnosing a weak or missing 1,6-RhaT. *A. sabaea* is F3′H-dominant (luteolin, kaempferol, and naringin high; apigenin absent) but is limited at the level of quercetin conjugation. *A. fleurentiniorum* is balanced across flavone and flavonol branches but lacks flavanone glycosides. *A. brunneodentata* retains a strong 3′-hydroxylation signature with modest glycosylation (luteolin > naringin ≈ rutin; apigenin and kaempferol not detected). *A. vera* produces moderate luteolin and kaempferol and some naringin but no rutin (rutinosylation bottleneck). *A. abhaica* is flavonol-only (kaempferol with some rutin), indicating absence of FNS activity and of flavanone 7-O-glycosylation.

To contextualize the enzyme-branch phenotypes, we mapped site-level climatic drivers across the collection localities (Fig. 6a–c). High-altitude, arid highlands (Al-

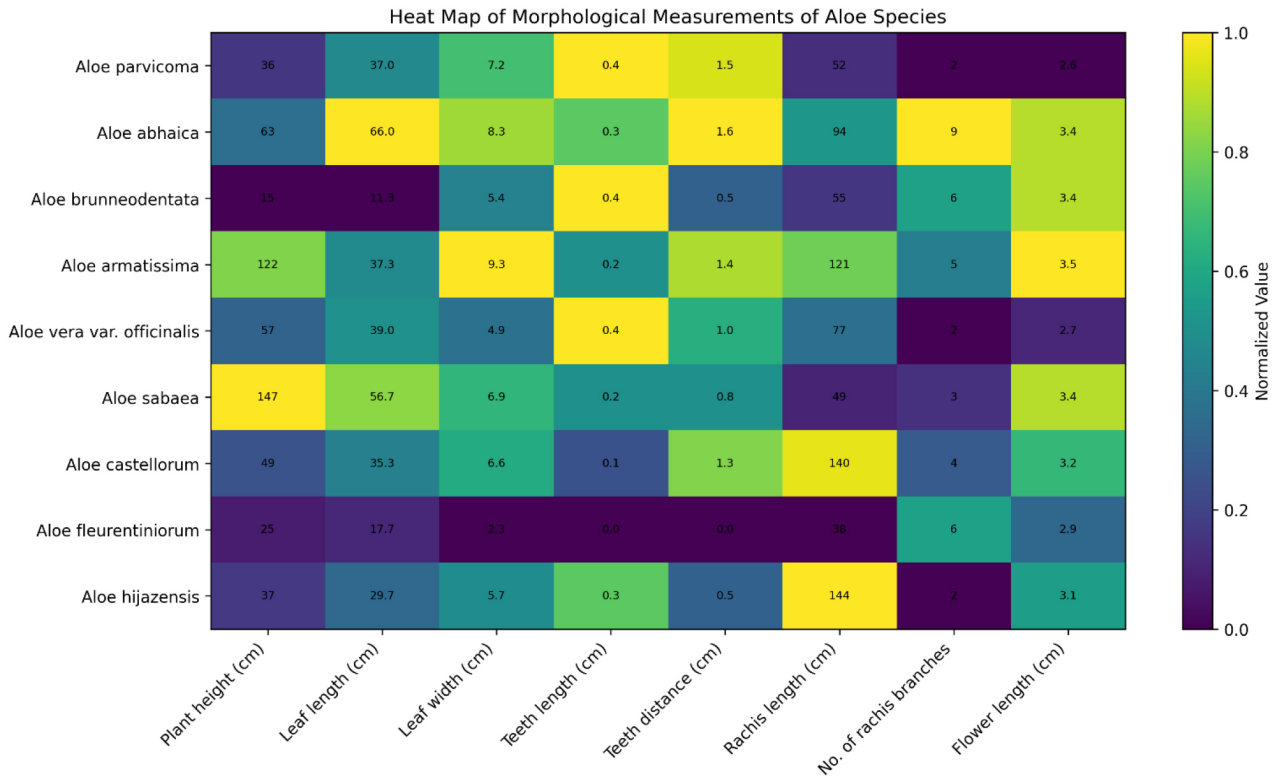

Fig. 3. Heat map of the normalized morphological metrics for the nine *Aloe* species examined.

Shafa, Bani Malik, South Taif, and Jabal Shada–Al Baha) cluster at UV index ≈9–10 with negligible rainfall, a regime that typically up-regulates F3′H/FLS-dependent flux and favors luteolin and kaempferol (and rutin where the 3-O-UGT→1,6-RhaT ladder is present). In contrast, more humid or mountain-shadowed locations (Wadi Ra'idah–'Asir; Jabal Fayfa–Jazan) show higher precipitation with moderate UV and temperatures, conditions consistent with stronger UGT/rhamnosyltransferase capacity and expansion of flavanone glycosides (e.g., naringin). Taif and Abha represent cooler, intermediate UV contexts. Together, these gradients modulate flux magnitude and end-point conjugation without altering the upstream PAL–C4H–4CL–CHS–CHI topology, thereby explaining the site-specific phenylpropanoid–flavonoid phenotypes described below.

3.5 Molecular Marker (RAPD-PCR)

Total genomic DNA was isolated from *Aloe* specimens collected at different locations. RAPD-PCR was performed using six oligonucleotides; only four primers produced reproducible bands. The agarose gel electrophoresis profiles generated by these four primers in the *Aloe* specimens are shown in Fig. 7. The data obtained from the analysis of these primers are summarized in Table 3, indicating a total of 22 reproducible bands and 14 polymorphic bands, corresponding to an overall polymorphism percentage of 64.16%.

Primer OPA-01 produced six bands with molecular weights ranging from 84.090 to 814.629 bp; three bands were polymorphic, and three were monomorphic. Primer OPA-13 produced five amplified bands with molecular weights ranging from 119.820 to 648.074 bp; three were polymorphic, and two were monomorphic. Primer OPB-17 produced six bands with molecular weights ranging from 95.332 to 443.186 bp, of which four were polymorphic and two were monomorphic. Primer OPD-15 produced five bands with molecular weights ranging from 2074.110 to 2260.390 bp, of which four were polymorphic and one was monomorphic.

Using the band frequency data from our RAPD scoring matrix across the nine *Aloe* species, we calculated the PIC values for each scorable locus per primer (Table 3). The mean PIC values in the range of 0.25–0.50 are typical for dominant RAPD markers employed at the interspecific level and indicate moderate informativeness, sufficient to support species-level discrimination [16,18]. Primers OPB-17 and OPD-15 showed the highest informativeness, consistent with their higher polymorphism percentages.

The RAPD-PCR analysis demonstrated significant genetic variation among the nine *Aloe* species examined from the Taif Highlands. Four decamer primers (OPA-01, OPA-13, OPB-17, and OPD-15) produced 22 bands, 14 of which were polymorphic, resulting in an overall polymorphism rate of 64.16%. This diversity exemplifies the adaptive ra-

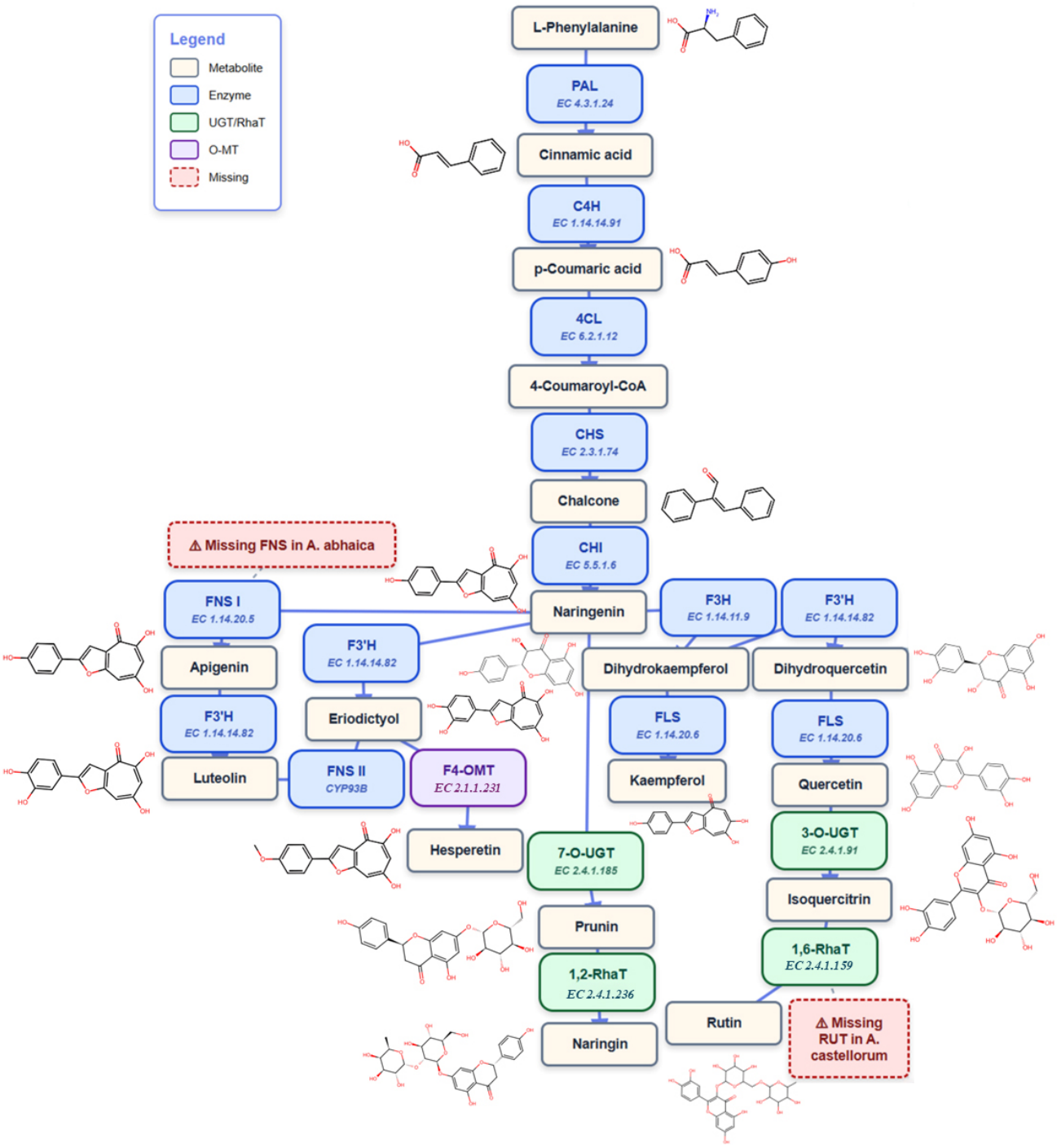

Fig. 4. Mechanistic map of *Aloe* flavonoid biosynthesis with enzyme EC numbers and conjugation modules. PAL–C4H–4CL–CHS/CHI establish the naringenin core; FNS I/II and F3′H define flavone output (apigenin, luteolin); F3H/FLS together with 3′-hydroxylation define flavonol output (kaempferol, quercetin); UGT78D2-like, rutinosyl transferase, 7-O-UGT, 1,2-rhamnosyltransferase, and F4′-OMT determine the accumulation of rutin, naringin, and hesperetin. EC, Enzyme Commission; PAL, phenylalanine ammonia-lyase; C4H, Butadiynyl; 4CL, 4-coumarate; CHS, chalcone synthase; CHI, chalcone isomerase; flavanone F3H, 3-hydroxylase; FLS, flavonol synthase; F3'H, flavonoid 3′-hydroxylase; UGT, UDP-glucuronosyltransferase; OMT, O-methyltransferases.

diation and ecological diversification inherent in the genus *Aloe*, which occupies a wide range of environments, from deserts to semi-humid locations [6,8]. Similarly, high levels of RAPD polymorphism have been documented in previous *Aloe* studies, validating the utility of this marker system for evaluating genetic diversity and elucidating interspecific relationships [16,17]. The clustering and similarity analyses reinforced species-level distinctions, grouping *A.*

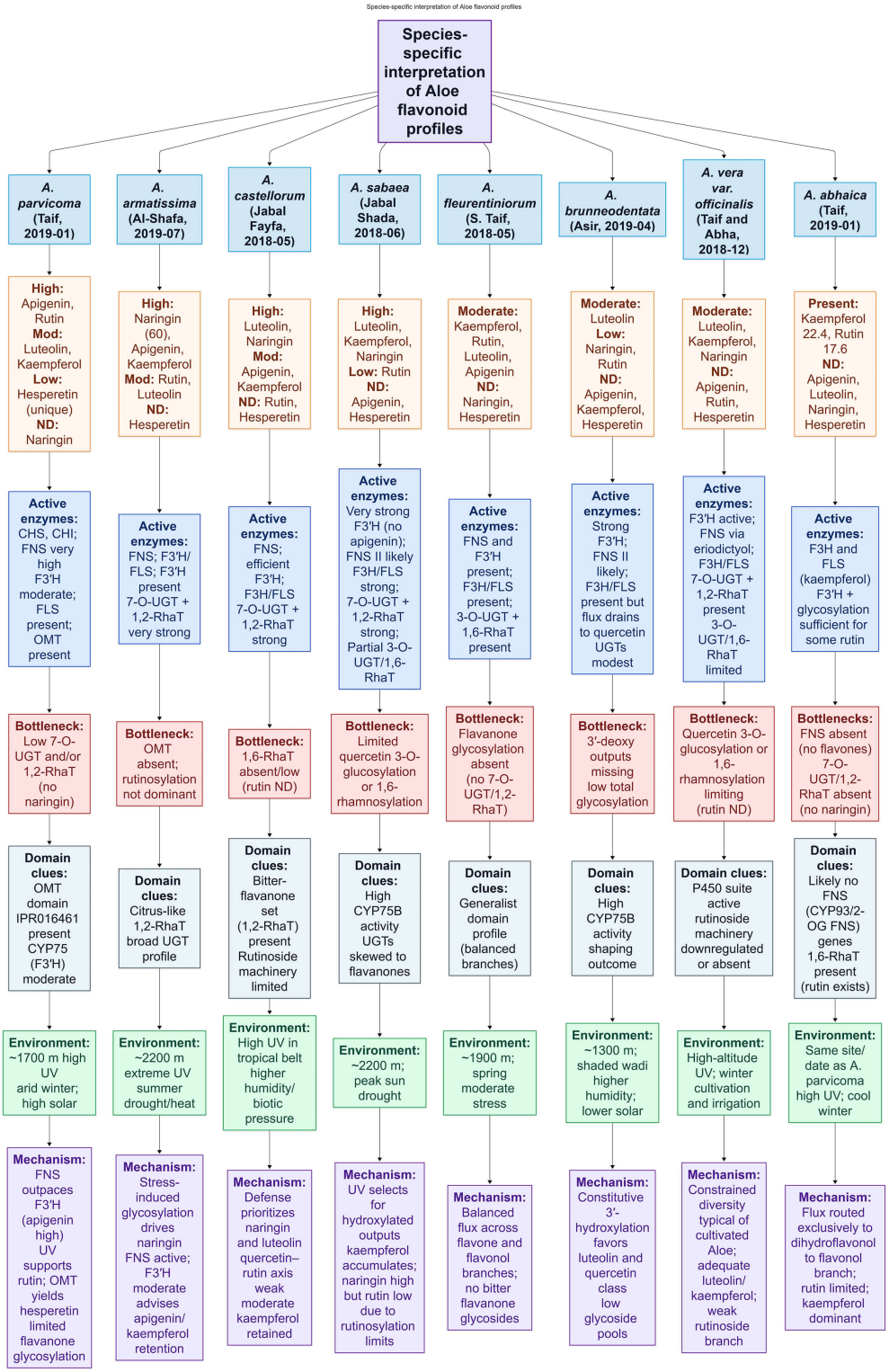

Fig. 5. ***Aloe*** **flavonoid network map of the enzyme-level and environmental regulation of apigenin, luteolin, kaempferol, rutin, naringin, and hesperetin**.

hijazensis and *A. brunneodentata* closely, whereas *A. parvicoma* exhibited genetic distinctiveness. These patterns may result from geographical isolation, genetic drift, and localized adaptation to distinct microclimates in the southwestern highlands. The RAPD data are congruent with the morphological and phytochemical findings, indicating that the examined *Aloe* taxa exhibit significant genetic differentiation, which underpins their phenotypic and metabolic diversity.

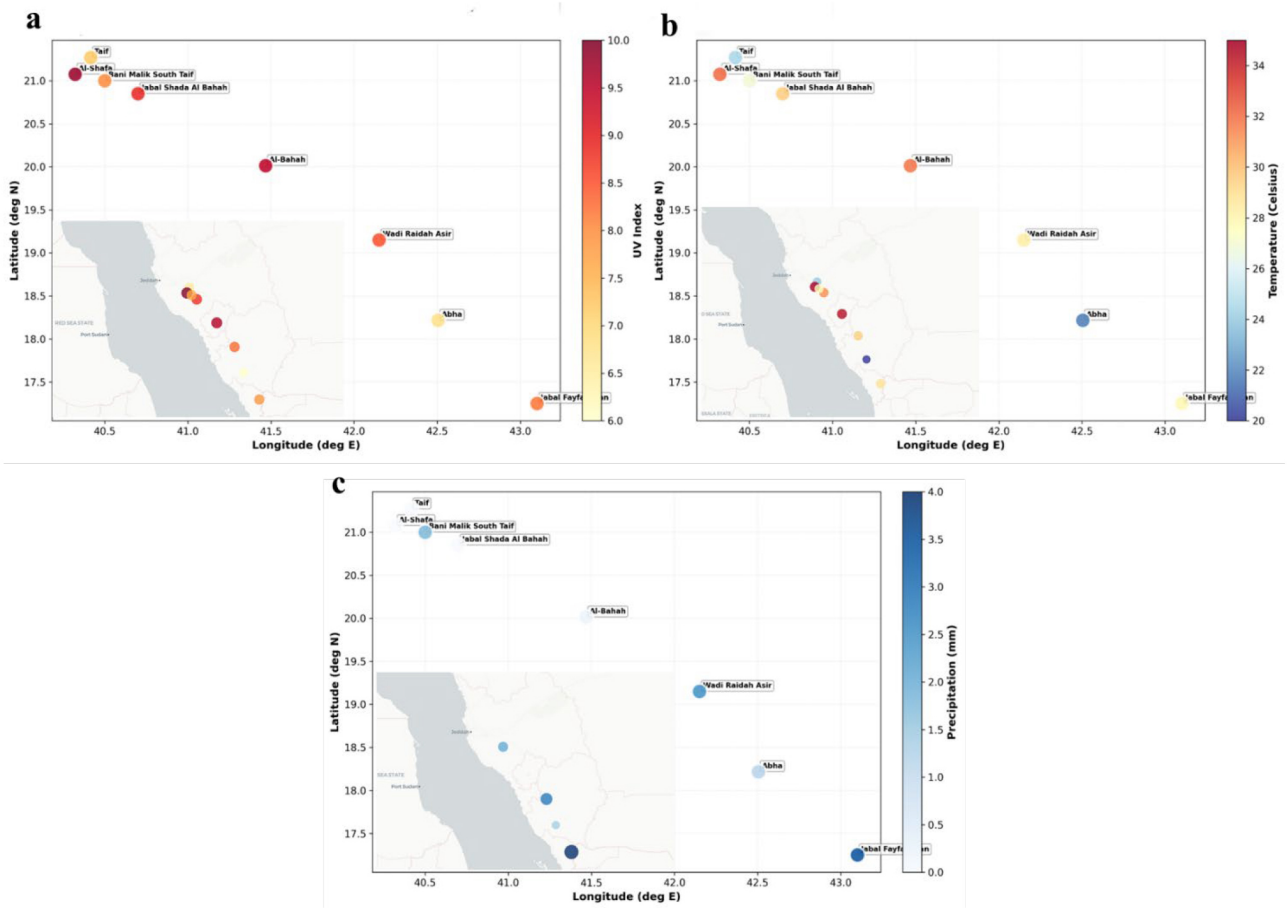

Fig. 6. Climatic contrasts across *Aloe* sites and expected effects on flavonoid routing. (a) Ultraviolet (UV) index, (b) temperature (°C), and (c) precipitation (mm) at sampling localities.

Table 3. Primer data and total polymorphism across the nine *Aloe* species.

No.	Code	Sequence (5′–3′)	Tm	Total bands	Polymorphic bands	Polymorphism (%)	Mean PIC*
1	OPA-01	CAGGCCCTTC	34	6	3	50	0.50
2	OPA-13	CAGCACCCAC	34	5	3	60.00	0.48
3	OPB-17	AGGGAACGAG	32	6	4	66.67	0.44
4	OPD-15	CATCCGTGCT	32	5	4	80	0.32
Total				22	14	64.16	0.435

*PIC, Polymorphism Information Content; Tm, melting temperature.

3.6 Similarity Analysis

The total similarity matrix clarified how the *Aloe* species are related to one another (Table 4). The highest similarity (58.62%) was recorded between *A. castellorum* and *A. fleurentiniorum*, followed by 55.50% between *A. abhaica* and *A. armatissima*, 52.77% between *A. sabaea* and *A. brunneodentata*, and 52.42% between *A. hijazensis* and *A. brunneodentata*.

Based on the molecular characterization of the nine *Aloe* species, the agglomerative clustering analysis indicated substantial differentiation among the taxa, with generally low similarity coefficients (Fig. 8; Table 4). According to the relatively higher similarity values, six clusters were distinguished: (A) *A. hijazensis* and *A. brunneodentata*; (B) *A. vera* var. *officinalis*; (C) *A. fleurentiniorum* and *A. castellorum*; (D) *A. sabaea*; (E) *A. abhaica* and *A. armatissima*; (F) *A. parvicoma*.

4. Discussion

The current study provides complementary lines of evidence for species discrimination and chemotaxonomic evaluation through an integrated assessment of the morphological, phytochemical, and molecular diversity of nine *Aloe* species found naturally in the Taif Highlands of Saudi Arabia. Different flavonoid accumulation patterns and RAPD-based genetic polymorphisms accompanied the observed interspecific variation in vegetative and reproduc-

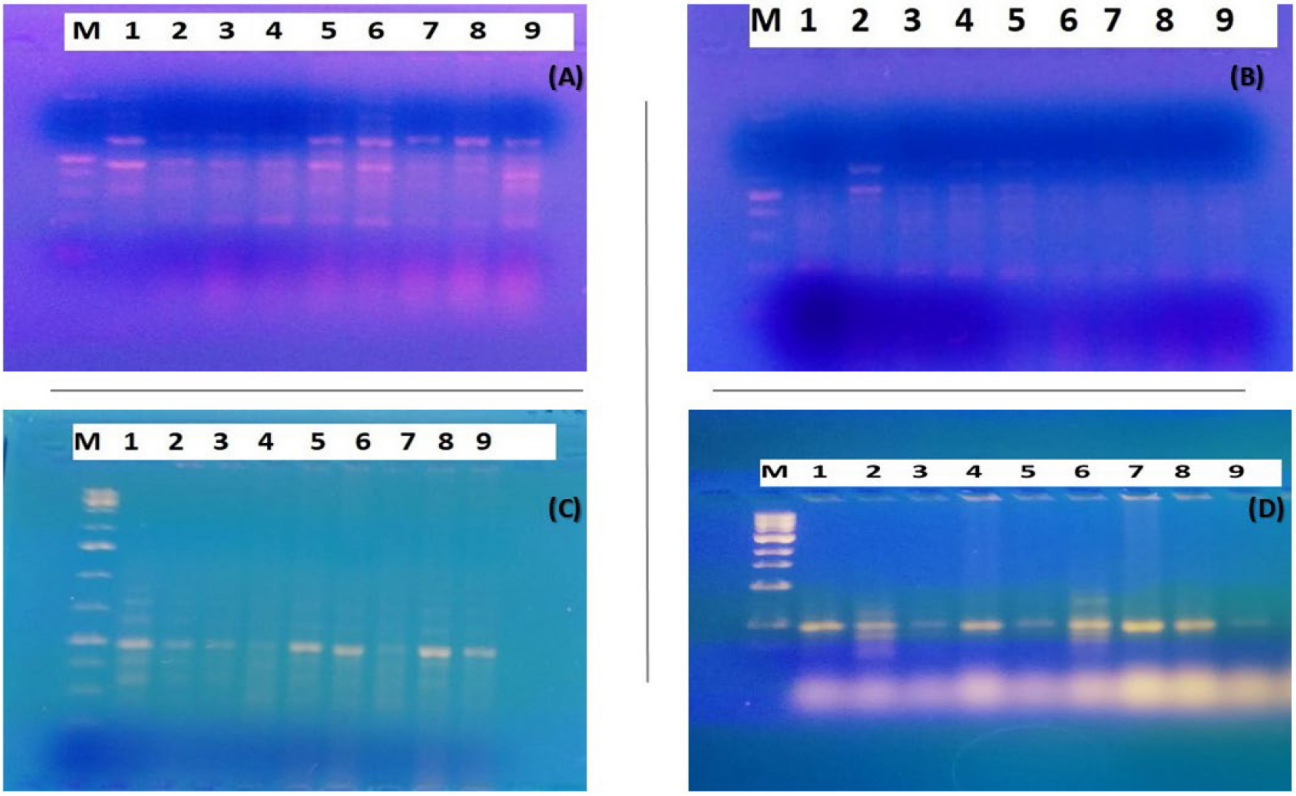

Fig. 7. Agarose gel profile of *Aloe* samples with four decamer primers (A: OPA-01, B: OPA-13, C: OPB-17, D: OPD-15). (Lanes 1: *Aloe hijazensis*; 2: *Aloe castellorum*; 3: *Aloe fleurentiniorum*; 4: *Aloe sabaea*; 5: *Aloe brunneodentata*; 6: *Aloe vera* var. *officinalis*; 7: *Aloe abhaica*; 8: *Aloe armatissima*; 9: *Aloe parvicoma*).

Table 4. Total similarity matrix between the nine study species based on their molecular characteristics.

	A. hij	*A. cas*	*A. fle*	*A. sab*	*A. bru*	*A. ver*	*A. abh*	*A. arm*
A. cas	34.32							
A. fle	41.25	58.62						
A. sab	35.75	30.15	33.02					
A. bru	52.42	49.82	47.30	52.77				
A. ver	36.55	32.37	31.83	27.75	40.17			
A. Abh	40.97	31.67	52.00	50.47	36.35	31.42		
A. arm	37.15	27.30	40.67	45.25	43.77	43.94	55.50	
A. par	33.90	20.92	35.67	43.90	35.47	22.90	41.97	48.80

A. hij, *Aloe hijazensis*; *A. cas*, *Aloe castellorum*; *A. fle*, *Aloe fleurentiniorum*; *A. sab*, *Aloe sabaea*; *A. bru*, *Aloe brunneodentata*; *A. ver*, *Aloe vera* var. *officinalis*; *A. abh*, *Aloe abhaica*; *A. arm*, *Aloe armatissima*; *A. par*, *Aloe parvicoma*.

tive traits, underscoring the complex interplay between genetic background and environmental adaptation in determining phenotypic and metabolic diversity. The metabolite profiles are consistent with differential flux pathways reported in plants exposed to diverse ecological conditions, even though flavonoid composition alone cannot directly indicate regulation of individual biosynthetic enzymes or genes. Similarly, the RAPD findings reinforce the observed morphological and phytochemical differences by demonstrating significant genetic divergence among the examined taxa. Collectively, these results show that combining phytochemical and molecular methods with classical taxonomy yields a more comprehensive understanding of *Aloe* biodiversity and provides valuable information for species identification, conservation planning, and the sustainable use of these economically and medicinally significant plants.

The nine *Aloe* species included in this study represent a purposively selected subset of the *Aloe* taxa documented in the Taif Highlands and surrounding southwestern highlands of Saudi Arabia. Species were selected based on documented occurrence in the region (Chaudhary [19]; Aseeri et al. [1]), accessibility of collection sites, and the availabil-

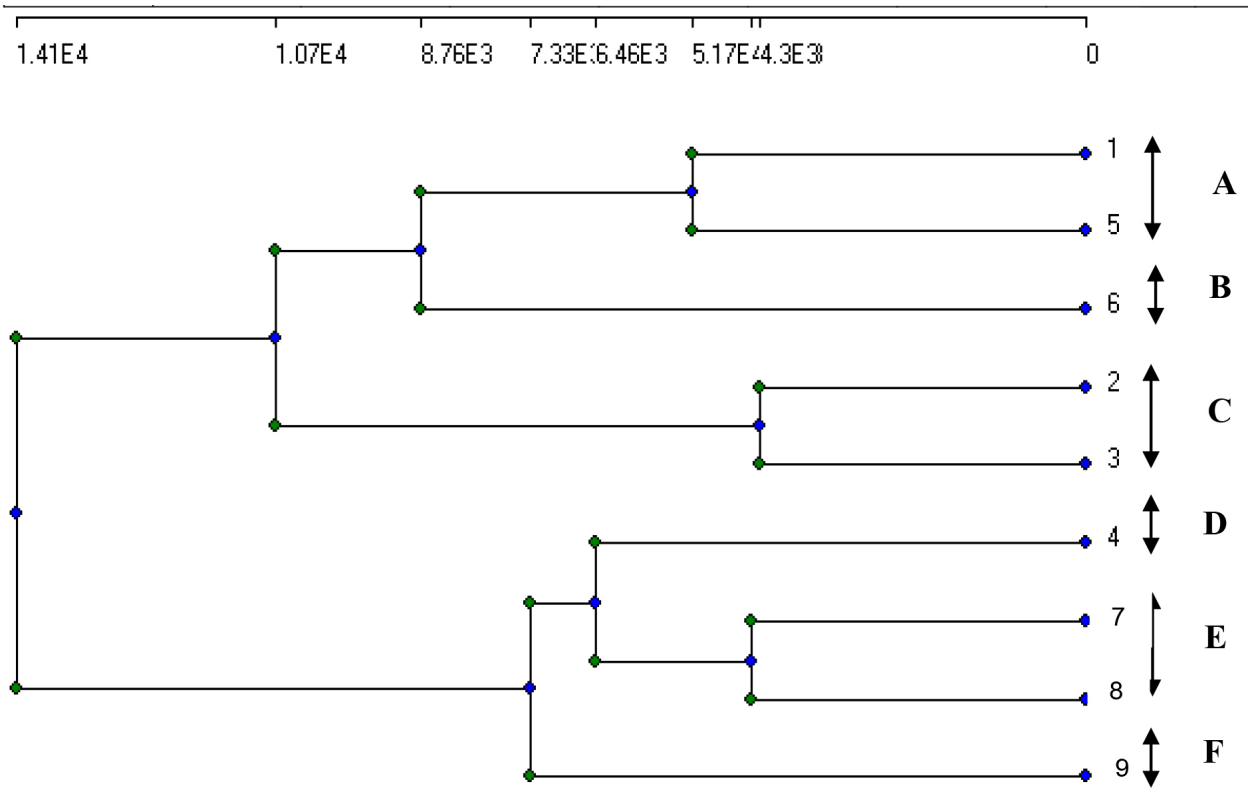

Fig. 8. Dendrogram of nine *Aloe* species collected from different locations, based on RAPD-derived molecular data. Species are numbered as follows: 1, *Aloe hijazensis*; 2, *Aloe castellorum*; 3, *Aloe fleurentiniorum*; 4, *Aloe sabaea*; 5, *Aloe brunneodentata*; 6, *Aloe vera* var. *officinalis*; 7, *Aloe abhaica*; 8, *Aloe armatissima*; 9, *Aloe parvicoma*. Fig. 8 illustrates the molecular relationships among the nine Aloe species based on RAPD-derived data and separates them into six distinct clusters. Group A includes *Aloe hijazensis* and *A. brunneodentata*, indicating a relatively close genetic relationship. Group B consists only of *A. vera* var. *officinalis*, reflecting its distinct molecular profile. Group C includes *A. fleurentiniorum* and *A. castellorum*, which showed the highest molecular similarity among the studied species, indicating a close genetic relationship. Group D consists of *A. sabaea* alone, demonstrating its molecular differentiation from the other taxa. Group E includes *A. abhaica* and *A. armatissima*, which showed relatively high genetic similarity. Finally, Group F consists only of *A. parvicoma*, indicating its distinct genetic profile and separation from the remaining *Aloe* species. Overall, the clustering pattern demonstrates substantial genetic differentiation among the nine studied Aloe species based on RAPD analysis.

ity of sufficient mature plant material at the time of field sampling. These species do not constitute an exhaustive floristic census of all *Aloe* taxa present in the region, and the findings of this study should be interpreted within this defined scope.

The interpretations presented in this discussion are based on quantitative morphological measurements, RAPD-derived genetic similarity data, and metabolite profiles identified by HPLC. Future research using transcriptomic, enzymatic, and experimentally controlled environmental datasets should formally test the pathway-level or environmental inferences proposed here, which are intended as hypothesis-generating interpretations consistent with the established literature rather than experimentally validated mechanistic conclusions.

This study also acknowledges several methodological limitations that must be considered when evaluating the results. Morphological characterization was conducted using three individuals per species, reflecting the limited availability of mature specimens among the nine *Aloe* taxa in the remote Taif Highlands. This small sample size inherently constrains the quantification of intraspecific phenotypic variability and reduces the statistical power of interspecific comparisons. Comparable limitations have been reported in morphological investigations of wild *Aloe* populations in the Arabian Peninsula, where species scarcity and habitat inaccessibility impose practical constraints on sampling [1,5].

The present study documented considerable variation in morphological features and vegetative growth among *Aloe* species, as well as differences in the presence and quantitative levels of their metabolites [11]. Moreover, morpho-chemical evaluations can provide insights into the genetic structure and diversity within and among species across different geographical regions, producers, and distributors [25]. Therefore, it was important to investigate

the genetic variation among these species. Morphological traits are both central to plant taxonomy and highly valuable in commercial use [26]. Environmental heterogeneity has led to phenotypic variation [27], making the application of genetic markers a suitable approach, as these markers have been successfully used to assess the structure of genetic variability and to establish genetic relationships among the investigated species [18].

The Agilent 1100 HPLC-MS system, equipped with a photodiode array detector and an electrospray ionization (ESI) source, facilitated the identification of flavonoids at 280 nm using gradient formic acid–acetonitrile solvent systems. This methodology ensured accurate profiling of key phytochemicals for comparative investigation among *Aloe* taxa [11]. External calibration standards were prepared for each of the seven target flavonoids (apigenin, luteolin, naringin, quercetin, rutin, kaempferol, and hesperetin) at six concentration levels spanning the expected analytical range (0.5, 1.0, 5.0, 10.0, 50.0, and 100.0 µg/mL), using commercially sourced reference standards of ≥95% purity (Sigma-Aldrich, Germany). Quercetin was used as the primary external standard for total flavonoid quantification, consistent with established HPLC protocols for *Aloe* phytochemical analysis [11].

4.1 Mechanistic Contextualization of Flavonoid Profiles

Pathway-anchored analysis offers a comprehensive framework for linking metabolite diversity in *Aloe* species to associated enzymatic and environmental factors. The phenylpropanoid–flavonoid biosynthetic pathway in *Aloe* begins with PAL and proceeds through several critical enzymes, including CHS, CHI, FNS I/II, F3H, FLS, and F3′H, followed by modifications catalyzed by glycosyltransferases (UGTs) and O-methyltransferases (OMTs) [24,28]. The absence or reduced activity of specific enzymes could be associated with differential regulation of flavonoid biosynthesis.

Flavonoids can inhibit or kill many bacterial strains, inhibit important viral enzymes such as reverse transcriptase and protease, and destroy certain pathogenic protozoans [13,29]. Flavonoids also act as antioxidants and radical scavengers, exerting protective effects against several diseases [30].

The environmental associations discussed below are presented as hypothesis-generating interpretations informed by the established literature on UV- and drought-induced regulation of flavonoid biosynthesis and should not be construed as statistically validated conclusions. Formal quantification of environment–metabolite relationships would require replicated population-level sampling across controlled environmental gradients, with directly measured microclimatic variables, and is recommended as a priority objective for future studies building on the present baseline characterization.

The investigation of natural plants and the isolation of their beneficial constituents are vital for controlling liver disease [31]. Flavonoids, including quercetin, kaempferol, rutin, and luteolin derivatives, enhance cellular defenses, thereby mitigating neuroinflammation and mitochondrial dysfunction [30]. According to Lin et al. [12], kaempferol is a well-characterized natural flavonol present in approximately 80% of plant-based foods, and its derivatives are strong antioxidants that help prevent oxidative damage to human cells, lipids, and DNA. In addition, quercetin and kaempferol neutralize free radicals and prevent oxidative damage [32] as well as reduce the likelihood of plant infection [33]. Moreover, numerous *in vitro* and *in vivo* studies have demonstrated the anticancer activity of kaempferol against various cancers, including breast [14,34], prostate [14], pancreas [35], lung [36], stomach, kidney [37], colon [38,39], bladder [40], and others.

An integrative evaluation of flavonoid biosynthesis in *Aloe* indicates that species-specific chemical profiles arise from the combination of key enzymatic branch points and the specificity of chemical modifications to those core flavonoid structures. The architecture of the flavonoid biosynthetic pathway is defined by competition for the central precursor to the pathway, naringenin, whose fate is ultimately determined by the relative activities of FNS, F3H, and FLS [24,28]. A further level of diversification of these core structures is achieved by other tailoring enzymes, such as F3′H, UGTs, and OMTs, which introduce functional groups into the flavonoid backbone, thereby modifying the molecular properties of the molecule [41,42].

Apigenin, a flavone, is produced directly by FNS activity, which converts naringenin to apigenin [43,44]. Alternatively, the flavonol route begins with the hydroxylation of naringenin by F3H to produce dihydrokaempferol (DHK), which is then oxidized to kaempferol by FLS [45,46]. A key modification is enzymatically mediated by cytochrome P450 F3′H, which introduces a 3′-hydroxyl group on the B-ring at the flavanone/dihydroflavonol stage, such as naringenin to eriodictyol and DHK to dihydroquercetin (DHQ), after which FLS converts DHQ to quercetin. Consequently, quercetin in the pathway depicted here is derived from DHQ via FLS, rather than formed by hydroxylation of kaempferol. This modification is often induced by external stimuli (e.g., UV radiation) and is generally mediated by environmental stress [24,28].

Final flavonoid products are usually stored as glycosides, which are water-soluble and are synthesized by UGTs that add a sugar moiety to the flavonoid core [47]. For example, rutin results from a two-step glycosylation of quercetin, whereas naringin, a bitter compound, is synthesized through a distinct cascade of glycosylation reactions acting on naringenin [48,49]. The presence of hesperetin indicates yet another modification pathway in which an O-methyltransferase adds a methyl group after 3’-hydroxylation [50,51]. Transcriptional regulation of

these pathways is tightly controlled by the MYB–bHLH–WD40 (MBW) complex, which modulates gene expression in response to developmental and environmental signals [52,53].

Therefore, the particular flavonoid composition detected in *Aloe* species can be viewed as the outcome of the respective enzymatic general capacity of *Aloe* species. For example, the complete absence of flavones in *A. abhaica* suggests either gene loss or silencing of the *FNS* gene, resulting in a complete shift in flux toward the production of flavonols, such as kaempferol, which also occurs in other monocots [54]. Conversely, the exceptionally high concentrations of naringenin observed in *A. armatissima* suggest increased glycosylation activity, potentially driven by gene duplication or transcriptional upregulation of specific 7-O-UGT and 1,2-rhamnosyltransferase enzymes [55].

The interaction between environmental factors and the functioning of these pathways is significant. In the high mountains of western Saudi Arabia, high levels of solar radiation and UV index can activate the ultraviolet-B (UV-B) radiation (280–315 nm) UVR8 photoreceptor pathway, thereby upregulating the expression of genes such as F3′H and FLS [56,57]. This pathway could help explain the high levels of 3′-hydroxylated flavonoids, including luteolin, and flavonols such as rutin in *Aloe* species from high-altitude locations, as these compounds function as effective UV screens [58,59]. In addition to solar radiation, drought and heat are common stressors in these high-mountain environments and may induce upregulation of UGTs, thereby contributing to a high pool of soluble glycosides that may participate in osmotic adjustment and complementary antioxidant defense [60,61]. More than mere speculation, this provides an initial framework for linking harsh climatic conditions to potentially elevated levels of glycosylated compounds, such as naringin, which was detected in species including *A. armatissima* and *A. castellorum* [62].

This integrated perspective demonstrates how genetic inheritance (the presence or absence of key enzyme genes) and environmental regulation (stress-induced modulation of enzyme activity) collectively shape the diverse phytochemical landscapes across the *Aloe* genus. Understanding these enzyme–compound relationships not only provides insight into plant adaptation but also opens avenues for biotechnological applications, where pathway enzymes could be targeted to enhance the production of medicinally valuable flavonoids in cultivated *Aloe* [63].

Phytochemical analyses involved HPLC profiling of species-level extracts with technical replication, adhering to standard practices in comparative phytochemical studies of wild-collected *Aloe* material [11,15]. However, the lack of multiple independently collected biological replicates per species constrains the statistical estimation of intraspecific chemical variability and should be addressed in future research by increasing field sampling across variable environments. The RAPD-PCR molecular analysis, conducted under reproducible conditions according to established protocols for *Aloe* [16], utilized a single DNA extraction per species. Consequently, the resulting diversity indices and clustering patterns represent species-level genetic profiles rather than population-level genetic structure estimates; comprehensive sampling across populations within each taxon is essential to elucidate phylogeographic relationships and adaptive divergence in this genus [18]. Despite these limitations, the convergence of morphological, phytochemical, and molecular clustering patterns across three independent datasets offers a mutually reinforcing evidence base that significantly enhances confidence in the interspecific groupings and ecological interpretations presented here. In total, 22 bands were obtained across all primers, resulting in a polymorphism percentage of 64.16% (Table 3). The CTAB-based extraction method and the RAPD conditions employed here have been effectively applied in *Aloe* species in multiple studies and can be further optimized (DNA quantity, Mg^{2+} concentration, primer concentration, annealing temperature) to enhance band clarity and reproducibility for the specified primers [16].

4.2 Limitations in Study

This study presents comprehensive morphological, phytochemical, and molecular characterizations of nine *Aloe* species from the Taif Highlands; nevertheless, several limitations must be considered when interpreting the results. Phytochemical analyses were performed on species-level extracts with few independent biological replicates, thereby limiting the ability to assess natural chemical heterogeneity within species. In addition, environmental interpretations linking flavonoid composition to climatic factors, including UV radiation, temperature, and precipitation, were inferred from established biosynthetic and ecological knowledge rather than validated through controlled experimental or transcriptomic analyses. Finally, the study focused on a selected subset of *Aloe* taxa accessible in the Taif Highlands and does not represent a complete floristic survey of all regional species. Future investigations incorporating larger population sizes, replicated sampling across environmental gradients, high-resolution genomic approaches, and functional analyses of flavonoid biosynthetic pathways will further strengthen understanding of the evolutionary, ecological, and chemotaxonomic diversity of *Aloe* species.

5. Conclusion

This study revealed significant morphological, phytochemical, and genetic diversity among nine *Aloe* species from the Taif Highlands in southern Saudi Arabia. Differences in leaf and flower morphology, together with distinct HPLC-derived flavonoid profiles, demonstrated clear chemotaxonomic distinctions among species. The pathway-anchored analysis elucidated mechanistic connections between metabolite composition, enzymatic fluxes in

the phenylpropanoid–flavonoid network, and environmental factors including UV exposure and precipitation. The pathway-informed interpretation of interspecific flavonoid variation and its proposed associations with environmental gradients should be viewed as hypothesis-generating conclusions, grounded in established biosynthetic and ecophysiological knowledge, that require future experimental validation through transcriptomic, enzymatic, and population-level ecological studies. Molecular analysis with RAPD-PCR verified a significant level of polymorphism (64.16%), affirming the genetic uniqueness and adaptive divergence of the examined species. Collectively, these findings underscore that *Aloe* species exhibit integrative diversity shaped by both genetic inheritance and ecological stress. This study provides essential baseline data for the taxonomy, conservation, and sustainable use of *Aloe* resources and lays the foundation for future molecular and metabolic engineering efforts to enhance the production of pharmacologically significant flavonoids.

Availability of Data and Materials

The data used to support the findings of this study are available from the corresponding author upon request.

Author Contributions

TG and ET designed the research study. TG, ET and SA performed the research. TG and SA conducted experiments. TG and ET wrote the initial draft of the manuscript. TG and ET analyzed the data. All authors contributed to editorial changes in the manuscript. All authors read and approved the final manuscript. All authors have participated sufficiently in the work and agreed to be accountable for all aspects of the work.

Ethics Approval and Consent to Participate

The plant materials of Aloe species were gathered from different Saudi Arbian location with personal permission. According to Saudian regulations and policies, this study does not involve human or animal subjects; therefore, ethical committee approval is not necessary.

Acknowledgment

The authors would like to acknowledge the Deanship of Graduate Studies and Scientific Research, Taif University for funding this work.

Funding

The authors would like to acknowledge the Deanship of Graduate Studies and Scientific Research, Taif University for funding this work.

Conflicts of Interest

The authors declare no conflicts of interest.

References

[1] Aseeri SA, Galal TM, Al-Yasi HM. Aloe species in the Kingdom of Saudi Arabia: morphological, phytochemical and molecular characterization. Lambert Academic Publishing Gmbh & Co.KG: Budapest, Hungary. 2020.

[2] Grace OM, Klopper RR, Smith GF, Crouch NR, Figueiredo E, Rønsted N, et al. A revised generic classification for Aloe (Xanthorrhoeaceae subfam. Asphodeloideae). Phytotaxa. 2013; 76: 7–14. https://doi.org/10.11646/phytotaxa.76.1.2

[3] Smith GF, Steyn EM. Taxonomy of Aloaceae. In Reynolds T (ed.) Aloes: The genus Aloe (pp. 15–30). CRC Press: Boca Raton, London, New York, and Washington, D.C. 2004.

[4] Klopper RR, Van Wyk AE, Smith GF. Phylogenetic relationships in the family Asphodelaceae (Asparagales). Biodiversity and Ecology/Schumannia. 2010; 3: 9–36.

[5] McCoy TA, Lavranos JJ. Two new species of Aloe from the Kingdom of Saudi Arabia. Cactus and Succulent Journal. 2014; 86: 258–263. https://doi.org/10.2985/015.086.0604

[6] Cousins SR, Witkowski ET. African aloe ecology: a review. Journal of Arid Environments. 2012; 85: 1–17. https://doi.org/10.1016/j.jaridenv.2012.03.022

[7] Gebremedhin AT. The types of Aloe species and their multifunction in Southern Ethiopia the cases of Hammer district. International Journal of Environmental Sciences & Natural Resources. 2017; 3: 91–94. https://doi.org/10.19080/IJESNR.2017.03.555619

[8] Smith GF, Steyn EA, Victor JE, Crouch NR, Golding J, Hilton-Taylor C. Aloaceae. Bothalia. 2000; 30: 206–211. https://doi.org/10.4102/abc.v30i2.560

[9] Smith GF, Van Wyk BE. Generic relationships in the Alooideae (Asphodelaceae). Taxon. 1991; 40: 557–581. https://doi.org/10.2307/1222765

[10] Galal TM, Aseeri SA, El-Midany MM. Comparative Phytochemical Analysis and Ethnopharmacological Potential of Nine Aloe Species Grown in the Western Highlands of Saudi Arabia. International Journal of Pharmacology. 2025; 21: 44072. https://doi.org/10.31083/IJP44072

[11] Galal TM, Aseeri SA, El-Midany MM. PRIMARY AND SECONDARY METABOLITE CONTRIBUTING TO THE CHEMOTAXONOMY OF NINE ALOE SPECIES GROWN IN SOUTHWESTERN HIGHLANDS OF SAUDI ARABIA. Applied Ecology & Environmental Research. 2025; 23: 3707–3720. http://dx.doi.org/10.15666/aeer/2302_37073720

[12] Lin CF, Leu YL, Al-Suwayeh SA, Ku MC, Hwang TL, Fang JY. Anti-inflammatory activity and percutaneous absorption of quercetin and its polymethoxylated compound and glycosides: the relationships to chemical structures. European Journal of Pharmaceutical Sciences: Official Journal of the European Federation for Pharmaceutical Sciences. 2012; 47: 857–864. https://doi.org/10.1016/j.ejps.2012.04.024

[13] Gouda HM. Phytochemical Studies on Opuntia littoralis Englem. at Wadi Maged - Matrouh [[MSc. Thesis]]. Faculty of Science, Helwan University: Cairo, Egypt. 2018.

[14] Halimah E, Diantini A, Destiani DP, Pradipta IS, Sastramihardja HS, Lestari K, et al. Induction of caspase cascade pathway by kaempferol-3-*O*-rhamnoside in LNCaP prostate cancer cell lines. Biomedical Reports. 2015; 3: 115–117. https://doi.org/10.3892/br.2014.385

[15] Añibarro-Ortega M, Pinela J, Barros L, Ćirić A, Silva SP, Coelho E, et al. Compositional Features and Bioactive Properties of *Aloe vera* Leaf (Fillet, Mucilage, and Rind) and Flower. Antioxidants (Basel, Switzerland). 2019; 8: 444. https://doi.org/10.3390/antiox8100444

[16] Deore P, Samantaray S, Maiti S. Genomic DNA isolation protocol for aloe barbadensis miller: using leaf gel for genetic charac-

terization. International Journal of Scientific and Research Publications. 2014; 4: 1–5.
[17] Rocco L, Valentino IV, Scapigliati G, Stingo V. RAPD-PCR analysis for molecular characterization and genotoxic studies of a new marine fish cell line derived from Dicentrarchus labrax. Cytotechnology. 2014; 66: 383–393. https://doi.org/10.1007/s10616-013-9586-y
[18] Andersen JR, Lübberstedt T. Functional markers in plants. Trends in Plant Science. 2003; 8: 554–560. https://doi.org/10.1016/j.tplants.2003.09.010
[19] Chaudhary H. Flora of the Kingdom of Saudi Arabia, Vol. II (pp. 342–354). Ministry of Agriculture and Water, National Herbarium, National and Water Research Center: Riyadh, Saudi Arabia. 2001.
[20] Hampl V, Pavlícek A, Flegr J. Construction and bootstrap analysis of DNA fingerprinting-based phylogenetic trees with the freeware program FreeTree: application to trichomonad parasites. International Journal of Systematic and Evolutionary Microbiology. 2001; 51: 731–735. https://doi.org/10.1099/00207713-51-3-731
[21] Hammer Ø, Harper DA, Ryan PD. PAST: Paleontological statistics software package for education and data analysis. Palaeontologia electronica. 2001; 4: 9.
[22] Jangpangi D, Patni B, Chandola V, Chandra S. Medicinal plants in a changing climate: understanding the links between environmental stress and secondary metabolite synthesis. Frontiers in Plant Science. 2025; 16: 1587337. https://doi.org/10.3389/fpls.2025.1587337
[23] Galal TM, Al-Yasi HM, Fawzy MA, Abdelkader TG, Hamza RZ, Eid EM, et al. Evaluation of the Phytochemical and Pharmacological Potential of Taif's Rose (*Rosa damascena* Mill var. *trigintipetala*) for Possible Recycling of Pruning Wastes. Life (Basel, Switzerland). 2022; 12: 273. https://doi.org/10.3390/life12020273
[24] Mao Y, Luo J, Cai Z. Biosynthesis and Regulatory Mechanisms of Plant Flavonoids: A Review. Plants (Basel, Switzerland). 2025; 14: 1847. https://doi.org/10.3390/plants14121847
[25] Moshrefi-Araghi A, Nemati H, Azizi M, Moshtaghi N, Shoor M. Association of Genetic Structure and Diversity in Iranian Wild Germplasms of Mentha longifolia L. Based on Phenotypical, Biochemical, and Molecular Markers. Chemistry & Biodiversity. 2021; 18: e2001044. https://doi.org/10.1002/cbdv.202001044
[26] López-Palacios C, Peña-Valdivia CB, Reyes-Agüero JA, Aguirre-Rivera JR, Ramírez-Tobías HM, Soto-Hernández RM, et al. Inter-and intra-specific variation in fruit biomass, number of seeds, and physical characteristics of seeds in Opuntia spp., Cactaceae. Genetic Resources and Crop Evolution. 2015; 62: 1205–1223. https://doi.org/10.1007/s10722-015-0223-9
[27] Kays SJ. Cultivated vegetables of the world: a multilingual onomasticon (Latin binomials and synonyms). Wageningen Academic. 2011; 3: 674–675. https://doi.org/10.3920/978-90-8686-720-2
[28] Liu W, Feng Y, Yu S, Fan Z, Li X, Li J, et al. The Flavonoid Biosynthesis Network in Plants. International Journal of Molecular Sciences. 2021; 22: 12824. https://doi.org/10.3390/ijms222312824
[29] Kumar P, Kumar D, Pal S, Singh S. Plant secondary metabolites in defense against phytopathogens: Mechanisms, biosynthesis, and applications. Physiological and Molecular Plant Pathology. 2025; 138: 102639. https://doi.org/10.1016/j.pmpp.2025.102639
[30] Etukudo EM, Usman IM, Oviosun A, Ojiakor VO, Jama IA, Makena W, et al. Exploring the phytochemical profile, antioxidant and anti-inflammatory potential of *Bidens pilosa*: A Systematic Review. Frontiers in Pharmacology. 2025; 16: 1569527. https://doi.org/10.3389/fphar.2025.1569527
[31] Saleem M, Irshad I, Baig MK, Naseer F. Evaluation of hepatoprotective effect of chloroform and methanol extracts of Opuntia monacantha in paracetamol-induced hepatotoxicity in rabbits. Bangladesh Journal of Pharmacology. 2015; 10: 16–20. https://doi.org/10.3329/bjp.v10i1.20825
[32] Gulcin İ, Alwasel SH. Metal ions, metal chelators and metal chelating assay as antioxidant method. Processes. 2022; 10: 132. https://doi.org/10.3390/pr10010132
[33] Laoué J, Fernandez C, Ormeño E. Plant Flavonoids in Mediterranean Species: A Focus on Flavonols as Protective Metabolites under Climate Stress. Plants (Basel, Switzerland). 2022; 11: 172. https://doi.org/10.3390/plants11020172
[34] Kim SH, Hwang KA, Choi KC. Treatment with kaempferol suppresses breast cancer cell growth caused by estrogen and triclosan in cellular and xenograft breast cancer models. The Journal of Nutritional Biochemistry. 2016; 28: 70–82. https://doi.org/10.1016/j.jnutbio.2015.09.027
[35] Liao W, Chen L, Ma X, Jiao R, Li X, Wang Y. Protective effects of kaempferol against reactive oxygen species-induced hemolysis and its antiproliferative activity on human cancer cells. European Journal of Medicinal Chemistry. 2016; 114: 24–32. https://doi.org/10.1016/j.ejmech.2016.02.045
[36] Yao S, Wang X, Li C, Zhao T, Jin H, Fang W. Kaempferol inhibits cell proliferation and glycolysis in esophagus squamous cell carcinoma via targeting EGFR signaling pathway. Tumour Biology: the Journal of the International Society for Oncodevelopmental Biology and Medicine. 2016; 37: 10247–10256. https://doi.org/10.1007/s13277-016-4912-6
[37] Kuo WT, Tsai YC, Wu HC, Ho YJ, Chen YS, Yao CH, et al. Radiosensitization of non-small cell lung cancer by kaempferol. Oncology Reports. 2015; 34: 2351–2356. https://doi.org/10.3892/or.2015.4204
[38] Song W, Dang Q, Xu D, Chen Y, Zhu G, Wu K, et al. Kaempferol induces cell cycle arrest and apoptosis in renal cell carcinoma through EGFR/p38 signaling. Oncology Reports. 2014; 31: 1350–1356. https://doi.org/10.3892/or.2014.2965
[39] Cho HJ, Park JHY. Kaempferol Induces Cell Cycle Arrest in HT-29 Human Colon Cancer Cells. Journal of Cancer Prevention. 2013; 18: 257–263. https://doi.org/10.15430/jcp.2013.18.3.257
[40] Dang Q, Song W, Xu D, Ma Y, Li F, Zeng J, et al. Kaempferol suppresses bladder cancer tumor growth by inhibiting cell proliferation and inducing apoptosis. Molecular Carcinogenesis. 2015; 54: 831–840. https://doi.org/10.1002/mc.22154
[41] He B, Bai X, Tan Y, Xie W, Feng Y, Yang GY. Glycosyltransferases: Mining, engineering and applications in biosynthesis of glycosylated plant natural products. Synthetic and Systems Biotechnology. 2022; 7: 602–620. https://doi.org/10.1016/j.synbio.2022.01.001
[42] Gan Y, Yu B, Liu R, Shu B, Liang Y, Zhao Y, et al. Systematic analysis of the UDP-glucosyltransferase family: discovery of a member involved in rutin biosynthesis in *Solanum melongena*. Frontiers in Plant Science. 2023; 14: 1310080. https://doi.org/10.3389/fpls.2023.1310080
[43] Tian S, Yang Y, Wu T, Luo C, Li X, Zhao X, et al. Functional Characterization of a Flavone Synthase That Participates in a Kumquat Flavone Metabolon. Frontiers in Plant Science. 2022; 13: 826780. https://doi.org/10.3389/fpls.2022.826780
[44] Pucker B, Iorizzo M. Apiaceae FNS I originated from F3H through tandem gene duplication. PloS One. 2023; 18: e0280155. https://doi.org/10.1371/journal.pone.0280155
[45] Tartik M, Liu J, Mohedano MT, Mao J, Chen Y. Optimizing yeast for high-level production of kaempferol and quercetin. Microbial Cell Factories. 2023; 22: 74. https://doi.org/10.1186/s12934-023-02084-4
[46] Chen Q, Song D, Sun X, Tian Y, Yan Z, Min T, et al. Func-

tional Characterization of F3H Gene and Optimization of Dihydrokaempferol Biosynthesis in *Saccharomyces cerevisiae*. Molecules (Basel, Switzerland). 2024; 29: 2196. https://doi.org/10.3390/molecules29102196

[47] Liu Y, Wang Q, Liu X, Cheng J, Zhang L, Chu H, et al. pUGTdb: A comprehensive database of plant UDP-dependent glycosyltransferases. Molecular Plant. 2023; 16: 643–646. https://doi.org/10.1016/j.molp.2023.01.003

[48] Wu QW, Wei M, Feng LF, Ding L, Wei WK, Yang JF, et al. Rhamnosyltransferases involved in the biosynthesis of flavone rutinosides in Chrysanthemum species. Plant Physiology. 2022; 190: 2122–2136. https://doi.org/10.1093/plphys/kiac371

[49] Xu H, Jiang Z, Lin Z, Yu Q, Song R, Wang B. FtUGT79A15 is responsible for rutinosylation in flavonoid diglycoside biosynthesis in Fagopyrum tataricum. Plant Physiology and Biochemistry: PPB. 2022; 181: 33–41. https://doi.org/10.1016/j.plaphy.2022.04.004

[50] Hanko EKR, Correia J, Souza CS, Green A, Chromy J, Stoney R, et al. Microbial production of the plant flavanone hesperetin from caffeic acid. BMC Research Notes. 2023; 16: 343. https://doi.org/10.1186/s13104-023-06620-8

[51] Pérez-Valero Á, Serna-Diestro J, Tafur Rangel A, Barbuto Ferraiuolo S, Schiraldi C, Kerkhoven EJ, et al. Biosynthesis of Hesperetin, Homoeriodictyol, and Homohesperetin in a Transcriptomics-Driven Engineered Strain of *Streptomyces albidoflavus*. International Journal of Molecular Sciences. 2024; 25: 4053. https://doi.org/10.3390/ijms25074053

[52] Jiang L, Gao Y, Han L, Zhang W, Fan P. Designing plant flavonoids: harnessing transcriptional regulation and enzyme variation to enhance yield and diversity. Frontiers in Plant Science. 2023; 14: 1220062. https://doi.org/10.3389/fpls.2023.1220062

[53] Cao Y, Mei Y, Zhang R, Zhong Z, Yang X, Xu C, et al. Transcriptional regulation of flavonol biosynthesis in plants. Horticulture Research. 2024; 11: uhae043. https://doi.org/10.1093/hr/uhae043

[54] Luo J, Luo C, Han M, Wang Q, Song Z, Zhang H, et al. A natural variation of flavone synthase II gene enhances flavone accumulation and confers drought adaptation in chrysanthemum. The New Phytologist. 2025; 247: 1445–1459. https://doi.org/10.1111/nph.70255

[55] Yuan Z, Li G, Zhang H, Peng Z, Ding W, Wen H, et al. Four novel *Cit7GlcTs* functional in flavonoid 7-*O*-glucoside biosynthesis are vital to flavonoid biosynthesis shunting in citrus. Horticulture Research. 2024; 11: uhae098. https://doi.org/10.1093/hr/uhae098

[56] Liu S, Gu X, Jiang Y, Wang L, Xiao N, Chen Y, et al. UV-B promotes flavonoid biosynthesis in *Ginkgo biloba* by inducing the *GbHY5-GbMYB1-GbFLS* module. Horticulture Research. 2023; 10: uhad118. https://doi.org/10.1093/hr/uhad118

[57] Wu W, Wu H, Liang R, Huang S, Meng L, Zhang M, et al. Light regulates the synthesis and accumulation of plant secondary metabolites. Frontiers in Plant Science. 2025; 16: 1644472. https://doi.org/10.3389/fpls.2025.1644472

[58] Agati G, Brunetti C, Dos Santos Nascimento LB, Gori A, Lo Piccolo E, Tattini M. Antioxidants by nature: an ancient feature at the heart of flavonoids' multifunctionality. The New Phytologist. 2025; 245: 11–26. https://doi.org/10.1111/nph.20195

[59] Koski M, Leonard E, Tharayil N. Foliar flavonoids across an elevation gradient: Plasticity in response to UV, and links with floral pigmentation patterning. Environmental and Experimental Botany. 2024; 106036. https://doi.org/10.1016/j.envexpbot.2024.106036

[60] Gharabli H, Della Gala V, Welner DH. The function of UDP-glycosyltransferases in plants and their possible use in crop protection. Biotechnology Advances. 2023; 67: 108182. https://doi.org/10.1016/j.biotechadv.2023.108182

[61] Dong G, Ma Y, Zhao S, Ma X, Liu C, Ding Y, et al. Rice glycosyltransferase DUGT2 enhances drought and salt tolerances through glycosylating a broad-spectrum of flavonoids under bZIP16 regulation. Plant Science: an International Journal of Experimental Plant Biology. 2025; 360: 112692. https://doi.org/10.1016/j.plantsci.2025.112692

[62] Salami M, Heidari B, Batley J, Wang J, Tan XL, Richards C, et al. Integration of genome-wide association studies, metabolomics, and transcriptomics reveals phenolic acid- and flavonoid-associated genes and their regulatory elements under drought stress in rapeseed flowers. Frontiers in Plant Science. 2024; 14: 1249142. https://doi.org/10.3389/fpls.2023.1249142

[63] Wang Y, Chen J, He G, Yin L, Liao Y. Unlocking the potential of flavonoid biosynthesis through integrated metabolic engineering. Frontiers in Plant Science. 2025; 16: 1597007. https://doi.org/10.3389/fpls.2025.1597007